International Journal of Pharmaceutics 395 (2010) 281–289

Contents lists available at ScienceDirect

International Journal of Pharmaceutics

journal homepage: www.elsevier.com/locate/ijpharm

Pharmaceutical Nanotechnology

Efficient overcoming of drug resistance to anticancer nucleoside analogs by nanodelivery of active phosphorylated drugs

Carlos M. Galmarini[b,1], Galya Warren[a], Madapathage T. Senanayake[a], Serguei V. Vinogradov[a,*]

[a] Department of Pharmaceutical Sciences, College of Pharmacy, and Center for Drug Delivery and Nanomedicine, University of Nebraska Medical Center, Omaha, NE 68198-6025, USA
[b] ENS-CNRS UMR 5239; UFR Lyon-Sud, 165 Chemin du Grand Revoyet, BP12 – 69921 Oullins, France

ARTICLE INFO

Article history:
Received 22 February 2010
Received in revised form 11 May 2010
Accepted 15 May 2010
Available online 24 May 2010

Keywords:
Drug resistance
Nucleoside analogs
Nucleoside 5′-triphosphate
Cationic nanogels
Tumor-targeting peptides
Xenograft tumor model

ABSTRACT

One of the major problems in cancer chemotherapy is the fast development of drug resistance to most anticancer therapeutics. Thus, an important cause of the eventual decline in clinical efficacy of cytotoxic nucleoside analogs was the selection of resistant cancer cells with deficiencies in the expression of nucleoside transporters or nucleoside-activating kinases. Here, we present an efficient strategy of overcoming this type of drug resistance by tumor-specific delivery of nanogel-encapsulated active triphosphates of nucleoside analogs (NATP). The small particles of biodegradable cationic nanogels loaded with anionic NATP efficiently interacted with cancer cells and released active drug compounds into the cytoplasm. The potential of novel drug formulations was evaluated in the nucleoside transport-deficient (CEM/araC/C8) or nucleoside activation-deficient (RL7/G) lymphogenic cancer cells. Compared to nucleoside analogs, NATP-loaded nanogels demonstrated increased cytotoxicity, reducing the drug resistance index 250- to 900-fold in CEM/araC/C8 cells and 70- to 100-fold in RL7/G cells. The strong cytotoxic effect of nanoformulations was accompanied by characteristic cell cycle perturbations, usually observed in drug-treated sensitive cells, and resulted in the induction of apoptosis in all studied drug-resistant cells. Efficient cellular accumulation of nanogels and the consequent increase in intracellular levels of NATP were found to be the major factors determining cytotoxic efficacy of nanoformulations. Decoration of nanogels with multiple molecules of tumor lymphatic-specific peptide (LyP1) enhanced the binding efficacy of nanocarriers with lymphogenic cancer cells. The targeted nanoformulation of activated gemcitabine (LyP1-NG-dFdCTP), when injected in subcutaneous RL7/G xenograft tumor model, demonstrated 2-fold more efficient tumor growth inhibition than gemcitabine at a higher dose. Nanogel-drug formulations exhibited no systemic toxicity during the treatment, hence extending the versatility of nucleoside analogs in the treatment of drug-resistant lymphogenic tumors.

1. Introduction

The cytosine analogs cytarabine (araC) and gemcitabine (dFdC) are cytotoxic anticancer drugs that interfere with nucleic acid synthesis either by incorporating into DNA and RNA, or by interfering with enzymes involved in nucleic acid synthesis, or by modifying the metabolism of physiological nucleosides (Ewald et al., 2008). Eventually, these activities induce strong inhibition of DNA replication and cell death. All nucleoside analogs share some common characteristics, such as cellular transport mediated by membrane transporters (Huber-Ruano and Pastor-Anglada, 2009) and mechanisms of intracellular activation into phosphorylated metabolites that interact with various cellular targets (Jordheim et al., 2003). Thus, the therapeutic efficiency of cytarabine and gemcitabine strongly depends upon intracellular accumulation of the corresponding nucleoside 5′-triphosphates. Unfortunately, some specific drug resistance mechanisms associated only with nucleoside analogs, such as deficiencies in the expression of human concentrative nucleoside transporter 1 (hENT1) or deoxycytidine kinase (dCK) enzyme, are capable of altering drug accumulation, metabolism, and activation, thereby reducing the intracellular concentration of active nucleoside 5′-triphosphates, and thus affecting the clinical efficacy of these drugs.

Various strategies have attempted to bypass bottlenecks in nucleoside transport and metabolism, circumventing drug resis-

Abbreviations: dFdC, gemcitabine; araC, cytarabine; NATP, 5′-triphosphate of nucleoside analogs; CTP, cytidine 5′-triphosphate; dCK, deoxycytidine kinase; hENT1, human concentrative nucleoside transporter 1; NG, nanogel; PEI, polyethylenimine; MAL, maleimide; NHS, N-hydroxysuccinimide; PEG, poly(ethylene glycol); PBS, phosphate-buffered saline; HPLC, high-performance liquid chromatography; SEC, size-exclusion chromatography.

* Corresponding author. Tel.: +1 402 559 9362; fax: +1 402 559 9543.
E-mail addresses: cmgalma@hotmail.com (C.M. Galmarini), vinograd@unmc.edu (S.V. Vinogradov).
[1] Current address: Cell Biology Department, Pharmamar SA, Madrid, Spain.

0378-5173/$ – see front matter © 2010 Elsevier B.V. All rights reserved.
doi:10.1016/j.ijpharm.2010.05.028

tance to nucleoside analogs (Galmarini et al., 2008a). One of the most advanced strategies, the pronucleotide approach, consists of the administration of biodegradable protected nucleoside 5′-phosphate derivatives. In fact, degradable lipophilic groups attached to the 5′-phosphate moiety mask the negative charge and result in neutral and membrane-permeable nucleotides. Some specific enzymatic cleavage or chemical activation of the masking group may be required for efficient intracellular delivery of pronucleotides (Peyrottes et al., 2004). However, this strategy is not free from serious disadvantages. Firstly, pronucleotides are degraded outside of cells due to esterase activity in the serum or tumor microenvironment. Secondly, the chemically driven release of active nucleotides from lipophilic phosphotriester precursors was not as easy as it seemed, due to the intermediate charged phosphodiester showing an extreme resistance to further chemical hydrolysis or enzymatic degradation. Finally, even an efficient release of phosphorylated nucleoside analogs from pronucleotides inside the cell would not be sufficient to attain cytotoxic activity if an intensive catabolic process was in operation, e.g. an overexpressed 5′-nucleotidase activity (Meier and Balzarini, 2006). Until now, these molecules have not shown any important antitumor activity in animal models, although some successful applications have been documented (Jordheim et al., 2004). Another approach included the restoration of nucleoside-activating enzymatic function (for example, dCK activity) by the transfection of drug-resistant cells (Jordheim et al., 2006). Various drug delivery systems, such as liposomes, nanoparticles, or erythrocytes, have also been evaluated for the delivery of nucleoside analogs in order to overcome deficiencies of intracellular transport or drug activation in tumor cells (Diab et al., 2007).

We have recently introduced a different type of hydrophilic drug carriers, biodegradable nanogels, consisting of cationic polymer networks, and explored their potential use for the delivery of nucleoside 5′-triphosphates in order to address the inadequate stability of these drug derivatives (Vinogradov et al., 2005a). In contrast to liposomes and polymeric micelles, which are dissociating quickly *in vivo* and release encapsulated drug molecules, nanogels are relatively stable and drug release from nanogel network can continue several days. This pattern presents more clinical advantages because the drug administration can be performed more rarely and the therapeutic effect will last for extended periods of time. Although biodegradable nanoparticles feature similar properties, their loading capacity for chargeable hydrophilic drugs is usually low. In addition, cationic nanogels were shown to enhance drug escape from endosomes, salvaging a significant part of active drug compounds from degradation in lysosomes (Vinogradov et al., 2005b). Nanogel-nucleoside 5′-triphosphate formulations demonstrated an equal or enhanced activity against breast and colorectal cancer cell lines *in vitro* and in a human breast tumor xenograft model (Galmarini et al., 2008b). Based on these encouraging results, we turned our attention to the application of active triphosphates of nucleoside analogs to the treatment of drug-resistant tumors. Here, we report for the first time our results on the efficient reversal of drug resistance to certain nucleoside analogs due to the deficiencies in drug transport/drug activation in lymphogenic cancer cells by these nanogel-drug formulations.

2. Material and methods

2.1. Materials

Clinical-grade cytarabine (araC, Aracytine®) was obtained from Pharmacia & Upjohn (St. Quentin, France). Clinical-grade gemcitabine (dFdC, Gemzar®) was obtained from Lilly (Hauts de Seine, France). Stock solutions of each drug were prepared in distilled water and fresh dilutions were prepared before each experiment. The corresponding nucleoside 5′-triphosphates araCTP and dFdCTP were synthesized by the one-pot method described previously (Vinogradov et al., 2005b). Propidium iodide, 3-[4,5-dimethylthiazol-2-yl]-2,5-diphenyl-tetrazolium bromide (MTT) and rhodamine isothiocyanate were purchased from Sigma–Aldrich (St. Louis, MO). [5-^{3}H]-Cytidine 5′-triphosphate (20–25 Ci/mmol) was acquired from Moravek Radiochemicals (Brea, CA). The bifunctional linker MAL-PEG$_{5000}$-NHS was obtained from GenKem Technology USA (Allen, TX). Peptides with N-terminal cystein and C-amide protection were custom synthesized by Biomer Technologies (Pleasanton, CA) and purified by semi-preparative reverse-phase HPLC. The tumor lymphatic-specific LyP1 peptide sequence, GNKRTRG (Laakkonen et al., 2002) and epidermal growth factor receptor-specific peptide sequence, MYIEALDSYA (Lutsenko et al., 2002) were used for nanogel modifications. All reagents were of analytical grade and used without purification.

Table 1
Particle size and drug loading of nanogel carriers.

Nanogel	Nanogel diameter (nm)[a]		Drug loading (μmol/mg)[b]		
	Unloaded	CTP-loaded	araCTP	dFdCTP	CTP
NG1	100 ± 8	58 ± 2	0.15	0.2	0.25
NG2	125 ± 6	64 ± 4	0.19	0.24	0.29

[a] Measured by dynamic light scattering. Data are shown: means ± SD (n = 3).
[b] Determined by UV absorbance in water using extinction coefficients for nucleosides.

2.2. Preparation of nanoformulations

As shown in Fig. 1, biodegradable nanogel NG1 consists of the crosslinked polymer network of PEG and the segmented polycation made of PEI (Mw 1800) connected by disulfide bonds (SS-PEI) (Vinogradov et al., 2006b; Kohli et al., 2007). Nanogel NG2 consists of a similar network but having a lipophilic poly(propylene oxide) core of Poloxamer P407 (Vinogradov et al., 2006a). Cytarabine (AraC) and gemcitabine (dFdC) were converted into 5′-triphosphates using the one-pot triphosphorylation protocol with minor modifications (Vinogradov et al., 2005b). The purity of NATP products was more or equal to 90% by ion-pair reverse-phase HPLC and UV spectrophotometric analysis. Nanogel formulations: NG1-araCTP, NG1-dFdCTP, NG2-araCTP, NG2-dFdCTP, NG1-CTP, and NG2-CTP (the last two used as a control without drug) have been obtained by mixing aqueous solutions of the corresponding nanogels and triphosphates; drug content and particle size of these nanoformulations can be found in Table 1. Triphosphate content in the lyophilized nanoformulations was measured spectrophotometrically. Tritium and rhodamine-labeled nanogels were synthesized using previously published protocols (Vinogradov et al., 2004).

LyP1 peptide-modified nanogel was prepared as follows. Nanogel NG1 (40 mg) was dissolved in 0.5 mL water, then a solution of a MAL-PEG$_{5000}$-NHS linker (2.5, 5 or 10 mg/0.5 mL) was added, and the mixture was incubated for 2 h at 25 °C. Without isolation, a 2-fold excess (1–4 mg) of LyP1 peptide was added in 0.5 mL DMF and the pH was reduced to 6 by 3 M sodium acetate, pH 5.5. The reaction was continued overnight at 4 °C. Peptide-modified nanogel was isolated by size-exclusion chromatography using a Sephacryl S-300 column equilibrated in 0.2 M sodium chloride, 20 mM sodium acetate, pH 6, in 20% ethanol. The product, LyP1-NG1, was desalted by dialysis (Mw cutoff 8–12 kDa) and lyophilized. Peptide content was determined using an automatic aminoacid analyzer (Applied Biosystems, Foster City, CA).

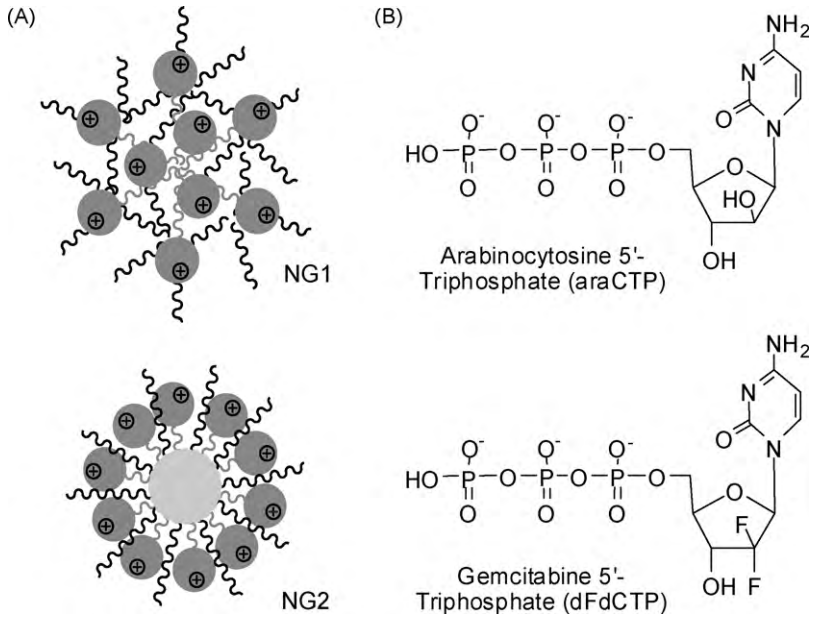

Fig. 1. (A) Schematic structures of cationic nanogel networks, NG1 (PEG-*cl*-SS-PEI) and NG2 (Poloxamer P407-*cl*-SS-PEI). Cationic PEI is colored in dark gray and hydrophobic Pluronic core in light gray. PEG molecules are shown as thin lines. (B) Chemical structure of 5′-triphosphates of cytotoxic nucleoside analogs: araCTP and dFdCTP.

2.3. Cell lines

The nucleoside transport-deficient drug-resistant cell line CEM/araC/8 was derived from human leukemic lymphoblast CCRF-CEM cells and characterized as described earlier (Ullman, 1989). This resistant variant was routinely cultured with 0.5 μM cytarabine and 0.25 μM tubercidin to maintain the mutant phenotype. The gemcitabine-resistant variant of the human follicular lymphoma cells, RL7/G, which demonstrated a reduced dCK level (Galmarini et al., 2004), was kindly provided by Dr. F. Bontemps (De Duve Institute, Bruxelles, Belgium). These cells were cultured in the presence of 2 μM gemcitabine. All cell lines were grown in RPMI containing 10% fetal calf serum, 1% L-glutamine and 2% penicillin–streptomycin at 37 °C in a humidified atmosphere containing 5% CO_2.

2.4. Cellular accumulation assays

A nanogel uptake assay was conducted in regular CEM and drug-resistant CEM/araC/C8 cells. Both cell lines were briefly incubated with rhodamine-labeled nanogels NG1 or NG2 for 1 h at 37 °C. Following centrifugation (650 rpm, 5 min), samples were washed twice with PBS, fixed in 1% paraformaldehyde (5 min, 20 °C) and counterstained with 5 μg/mL Hoescht 33258. Fluorescent images were captured using a fluorescence microscope (Axioplan II; Zeiss, Oberkochen, Germany) and processed using an ISIS/mFISH imaging system (Metasystems, Germany).

Intracellular levels of dFdCTP were analyzed in the total triphosphate pool by analytical ion-pair HPLC. Briefly, gemcitabine-resistant RL7/G cells (2×10^6) were treated with nanogel-dFdCTP formulations (3.5 mg/mL, 4 h at 37 °C) in the medium containing 10% serum and 2 μM gemcitabine. Total triphosphates were isolated from cells following the treatment with 400 μL of cold 10% trichloroacetic acid (20 min, 4 °C). Cell debris was precipitated by centrifugation (15,000 rpm, 10 min at 4 °C), and the supernatant was transferred into sterile tubes and extracted three times with 600 μL of the cold mixture of trioctylamine-freon, 1:4 (v/v). The aqueous phase was transferred into clean tubes, spiked with 10 μM ATP and 10 μM CTP, and precipitated with 2% sodium perchlorate in acetone (20 min at −20 °C). The precipitate was washed with acetone, dried, and analyzed by analytical ion-pair HPLC as previously described (Galmarini et al., 2008b).

2.5. Cytotoxicity assay

Cytotoxicity was determined using an MTT assay (Twentyman et al., 1989). Cells were incubated with different concentrations of nanoformulations in complete medium for 72 h at 37 °C, then the medium was renewed and cells were treated with MTT (4 mg/mL) for 4 h at 37 °C. The purple formazan product forming in living cells was dissolved by cell treatment with DMSO (0.1 mL) and quantified by absorbance at 560 nm. Positive and negative controls included wells with untreated cells or medium containing MTT with no cells, respectively. Chemosensitivity was expressed as the effective drug concentration inhibiting cell proliferation by 50% (IC_{50}) and was determined from drug concentration–effect curves using GraphPad Prism 4.03 software (GraphPad, San Diego, CA).

2.6. Cell cycle distribution analysis

For analysis of DNA content and cell cycle distribution, CEM, CEM/araC/C8, RL7 and RL7/G cells were treated with 1 μM solutions of cytarabine, gemcitabine, or corresponding solutions of NG1-araCTP, NG2-araCTP, NG1-dFdCTP and NG2-dFdCTP formulations for 24 h. After drug-exposure, 10^6 cells/mL were resuspended in 2 mL of propidium iodide solution (50 μL/mL), incubated for 1 h at 4 °C and then analyzed by flow cytometry (FACScalibur, Becton Dickinson, San Jose, CA). Cell cycle distribution and DNA ploidy status was calculated after exclusion of cell doublets and aggregates on an FL2-area/FL2-width dot plot using FlowJo 7.2.2 (Treestar, Ashland, OR).

2.7. Apoptosis analysis

The apoptotic fraction was determined using the Annexin-V-Fluos Staining Kit (Boehringer Mannheim, Germany). For this purpose, CEM, CEM/araC/C8, RL7 and RL7/G cell lines were treated with 1 μM cytarabine, gemcitabine, or corresponding NG1-araCTP, NG2-araCTP, NG1-dFdCTP and NG2-dFdCTP formulations for 24 h and then processed according to the manufacturer's protocol. Flow

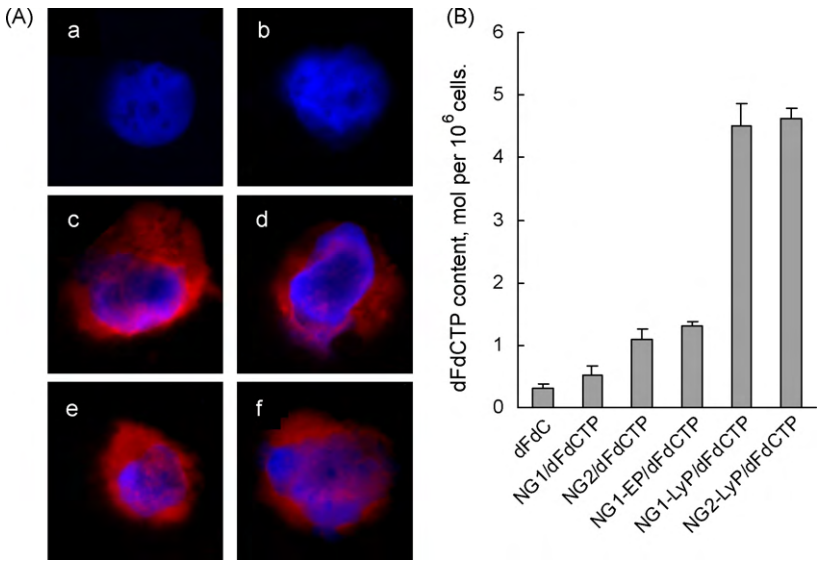

Fig. 2. Cellular uptake of nanogels in drug-resistant cancer cells. (**A**) CEM/araC/C8 (left panel) and CEM (right panel) cancer cells (a and b: non-treated control) were treated with rhodamine-labeled nanogels NG1 (c and d) or NG2 (e and f) for 1 h at 37 °C. Nuclei were counterstained with Hoechst 33258 dye. (**B**) Cellular accumulation of dFdCTP in drug-resistant RL7/G follicular lymphoma cells. Cells were incubated with 2 μM gemcitabine and drug nanoformulations with equal concentrations of dFdCTP for 4 h at 37 °C. Total nucleoside triphosphate pool was isolated, and dFdCTP content was quantitatively analyzed by ion-pair HPLC. Results are normalized by number of treated cells and shown as data ± SEM ($n = 3$).

cytometry analysis was performed as described in the previous section.

2.8. Tumor xenograft experiments

Gemcitabine-resistant RL7/G cells (1×10^6 per injection) were suspended in medium containing 20% Matrigel (BD Bioscience, San Jose, CA) and inoculated subcutaneously in the right flank of athymic BALB/c *nu/nu* mice (code 088, Charles River Laboratories, Wilmington, MA). As soon as small subcutaneous tumors were palpable, the mice were randomly separated into groups of five animals each. Initially, accumulation of [^{3}H]-CTP-loaded nanogels with various degrees of modification by LyP1 peptide was studied. Equal doses of each nanogel, non-modified and decorated with 1, 2 or 4 wt% LyP1, were injected via the tail vein, and accumulation of radioactivity in tumors was measured 16 h later. The collected tumors were homogenized in Solvable™ tissue solubilizer (Perkin-Elmer, Downers Grove, IL). Radioactivity of samples was measured in an Ultima Gold scintillator (Sigma) and normalized by the weight of tumors.

For *in vivo* tumor growth inhibition experiments, only NG1 nanogels, naked or modified with LyP1 peptide (4%, w/w), were used. Well-tolerated doses of NG1-dFdCTP formulations (60 mg/kg, 10 wt% gemcitabine) and gemcitabine (12 mg/kg) were injected into the tail veins of mice with subcutaneous RL7/G tumors twice a week over a 30-day period. Tumors were measured with calipers and tumor volume was calculated using the equation $V = 1/2\, a^2 b$, where a and b are the tumor width and length. Body weight loss was controlled among the groups throughout the experiment. Spleen and liver size was also compared in groups treated with gemcitabine or drug nanoformulations. Statistical analysis was performed by application of the two-tailed unpaired t-test (differences with $P < 0.05$ were considered significant) and F-test to compare variances in groups using the GraphPad Prism 4.03 software.

3. Results

3.1. Preparation of nanogel formulations

Biodegradable nanogels NG1 (PEG-*cl*-SS-PEI) and NG2 (P407-*cl*-SS-PEI) have been synthesized by an emulsification–solvent evaporation method and characterized by elemental analysis, ^{1}H NMR and potentiometric titration as previously described (Vinogradov et al., 2005a). At neutral pH, these nanogels could encapsulate from 0.15 to 0.29 μmol of NATP per 1 mg of nanoformulation (Table 1). The white solid lyophilized products could be easily redissolved in aqueous media and formed stable transparent dispersions with low hydrodynamic diameter (61 ± 3 nm) that did not show any time-dependent changes. The diameter of drug-loaded nanogels was dropped nearly 2-fold, and zeta-potential of drug nanoformulations was decreased from 26 ± 3 mV for non-loaded nanogels to near-zero value (4.2 ± 3.4 mV, $n = 3$). This effect demonstrated formation of core-shell particles having a dense core of the NATP–PEI complex and polymeric shell consisting of PEG molecules. This PEG shell covers the surface of particles and shields particle charge, reducing zeta-potential. This particle architecture is optimal for systemic drug delivery in order to prevent binding of serum proteins and the consequent capture of circulating nanoparticles by macrophages.

LyP1 peptide-decorated nanogels were synthesized by a one-pot procedure, including nanogel modifications with MAL-PEG-NHS linker and, then, with the 2-fold excess of thiolated peptide. The surface-modified nanogels have been isolated by size-exclusion chromatography (SEC), and the peptide content was determined by amino acid analysis after acidic hydrolysis of samples. On average, the peptide content calculated from these data was equal to 0.85 (LyP 1%), 1.9 (LyP 2%) and 3.5 (LyP 4%), which corresponded to nearly 90% conversion of the nanogel into LyP1-conjugate.

3.2. Drug accumulation

The rhodamine-labeled nanogels rapidly accumulated in regular and drug-resistant cancer cells, showing mostly cytoplasmic distribution after 1 h incubation (Fig. 2A). No principal difference between nanogels NG1 and NG2 was observed in their intracellular distribution. The major portion of nanocarriers was initially accumulated in the endosomes (Nori and Kopecek, 2005). Drug release from nanogels can be initiated by the acidification of endosomes, or as the result of drug substitution in nanogel networks with other anionic compounds such as the phospholipids of the

Table 2
Cytotoxicity of nucleoside analogs and triphosphate drug-loaded nanogels in regular and drug-resistant cancer cells.

Drug (μM)	CEM	CEM/araC/C8	Resistance index	RL7	RL7/G	Resistance index
Cytarabine	0.01 ± 0.003	>100	>10,000	0.74 ± 0.09	>100	135
NG1-araCTP	0.1 ± 0.08	1.2 ± 0.6	12	1.7 ± 0.1	2.3 ± 0.7	1.4
NG2-araCTP	0.17 ± 0.1	4 ± 1.5	24	4.7 ± 0.3	6 ± 2	1.3
Gemcitabine	0.01 ± 0.004	39 ± 10	3900	0.02 ± 0.009	24.3 ± 3	1215
NG1-dFdCTP	0.17 ± 0.09	2.5 ± 0.6	15	0.4 ± 0.2	5.1 ± 0.2	13
NG2-dFdCTP	0.18 ± 0.09	2.9 ± 0.6	16	0.23 ± 0.07	4.2 ± 0.6	18
NG1-CTP	19.3 ± 1	18.3 ± 3	n/a	55 ± 0.7	57 ± 0.7	n/a
NG2-CTP	17 ± 0.1	23 ± 0.6	n/a	25 ± 0.4	28.5 ± 4.9	n/a

IC_{50} values (μM, calculated by drug content) represent means ± SD of three separate experiments.

cellular membrane. Membranotropic properties of nanogels and the effect of nanogel binding with the cellular membrane on drug release have been previously documented (Vinogradov et al., 2005b). In the next step, we directly analyzed dFdCTP accumulation in drug-resistant RL7/G cells after the treatment with various nanogel-dFdCTP formulations (Fig. 2B). The inherent level of gemcitabine phosphorylation was very low in RL7/G cells; therefore, the delivery of nanoformulated dFdCTP would increase drug concentration up to the level when apoptosis starts. In these cells, drug transport was not affected; however, the conversion of gemcitabine into dFdCTP was deficient. A quantitative ion-pair HPLC analysis of dFdCTP in the total cellular triphosphate pool isolated from nanogel-dFdCTP-treated cells was then performed. As shown in Fig. 2B, a low initial level of intracellular dFdCTP in RL7/G cells cultivated in the presence of 2 μM gemcitabine was increased 2–4 times after a short treatment with dFdCTP-loaded nanogels. Nanogel NG2 demonstrated 2 times higher drug delivery efficiency than NG1. It is well known that an *in vitro* cellular uptake of nanogel particles having low buoyant density strongly depends upon interactions with the surface of treated cells. Previously, we demonstrated that fully loaded nanogels had shown weak interactions with the cell surface, while partially loaded (i.e. positively charged) or properly vectorized nanogels demonstrated efficient binding (Vinogradov et al., 2004). Evidently, non-modified NG2 was bound more efficiently than NG1 following 4 h incubation with RL7/G cells, because it has resulted in 2-fold increase of dFdCTP accumulation compared to free gemcitabine treatment. This was in agreement with our earlier results on the higher cellular uptake of Pluronic-based nanogels (Vinogradov et al., 2006a). All peptide-decorated nanogels (peptide content: 4 wt%) increased intracellular levels of dFdCTP. No statistically significant difference between LyP-NG1 and LyP-NG2 was determined. It may reflect the fact that surface decoration with PEG molecules could shield the effect of hydrophobic polymer in inner core, making both nanogels equivalent in their receptor-mediated cell binding. While the effect of the EGFR-specific peptide (EP) was ca. 4-fold, tumor lymphatic-specific peptide (LyP1) induced a nearly 14-fold increase in observed dFdCTP levels. In our conditions, both LyP1 peptide-modified nanogels were found equally efficient in binding to the follicular lymphoma RL7/G cells.

3.3. Cell growth inhibitory assay

In regular CEM and RL7 cell lines, triphosphate drug-loaded nanogels showed higher IC_{50} values than nucleoside analogs (Table 2). CEM-araC/C8 and RL7/G cells were 10,000-fold and 135-fold more resistant to cytarabine and 3900-fold and 1215-fold more resistant to gemcitabine, respectively. The drug resistance index was calculated as a ratio of IC_{50} values obtained in drug-resistant and regular cells. After the treatment with NG1-araCTP, NG2-araCTP, NG1-dFdCTP and NG2-dFCTP, the drug-resistant CEM-araC/C8 cells have become in average 500–1000 times and 250 times more sensitive than following the treatment with cytarabine and gemcitabine, respectively. Likewise, the treatment of drug-resistant RL7/G cells with nanoformulations resulted in drug resistance index reduction of 100 times and 70–100 times compared to cytarabine and gemcitabine, respectively. Control experiments with nanoformulations of the nontoxic CTP demonstrated levels of the intrinsic cytotoxicity of cationic nanogels and were very close in sensitive and drug-resistant cells. All these data indicate that nanogels carrying the active triphosphate form of cytarabine or gemcitabine are able to significantly reverse the drug-resistant phenotype of CEM/araC/C8 and RL7/G cancer cell lines.

3.4. Cell cycle distribution analysis

Since the triphosphate drug-loaded nanogels could induce cell cycle perturbations in sensitive and drug-resistant cells, we compared cell cycle distribution in both types of treated cells by flow cytometry (FACS). As shown in Table 3, treatment of sensitive CEM cells with araC induced accumulation of cells in the DNA replication phase (S-phase) and inhibited cell division (G2/M), while gemcitabine increased cell accumulation in growth phase (G0/G1) associated with inhibition of cell division (G2/M). Treatment with nanoformulations resulted in the comparable strong accumulation in G0/G1 phase and inhibition of cell division. However, treatment of drug-resistant CEM/araC/C8 cells with araC showed no inhibition of cell division. Compared to the free drug, araCTP-nanogels induced cell accumulation in G0/G1 phase, an arrest of DNA replication (S-phase), and medium inhibitory effect on cell division (G2/M). Effect of dFdCTP-nanoformulations was opposite on G0/G1 and S-phases. In sensitive RL7 cells, both nucleoside analogs significantly inhibited cell division, reducing also DNA replication (S-phase). Nanoformulations demonstrated the same pattern. Treatment of drug-resistant RL7/G cells with both nucleoside analogs did not induce any cell cycle perturbations as compared to non-treated cells. In contrast, araCTP-nanogels induced strong growth inhibition (G0/G1) and cell accumulation within the DNA replication phase, although cell division was not inhibited. All dFdCTP-nanogels induced a significant cell accumulation within the cell growth phase (G0/G1) on the level observed in the sensitive RL7 cells at the expense of DNA replication (S-phase). Cell division (G2/M) was also significantly inhibited. All these results demonstrated that nanoformulations of activated triphosphates of nucleoside analogs have been able to induce cell cycle perturbations in drug-resistant cell lines, in many aspects similar to effects observed in sensitive cells after the treatment with nucleoside analogs.

3.5. Apoptosis detection

Nanoformulation-induced apoptosis was studied by Annexin-V flow cytometry (Table 4). In sensitive cells, treatment with nucleoside analogs caused an increase in Annexin-V staining, which is typical of the induction of apoptosis. Drug-resistant CEM/araC/C8 and RL7/G cells exhibited much lower levels of apoptosis after treat-

Table 3
Cell cycle distribution in parental and drug-resistant cancer cells after treatment with nucleoside analogs or triphosphate-loaded nanogels (FACS data).

Cell/phase[a]	Control	araC	NG1-araCTP	NG2-araCTP	dFdC	NG1-dFdCTP	NG2-dFdCTP
CEM							
G0/G1	49 ± 2	46 ± 8	65 ± 0.3	66 ± 3	68 ± 6	76 ± 5	77 ± 2
S-phase	44 ± 4	50 ± 10	34 ± 0.3	34 ± 6	30 ± 7	24 ± 7	23 ± 7
G2/M	5.7 ± 3	2 ± 5	1.5 ± 0.3	1.9 ± 0.9	1 ± 1	1.6 ± 0.2	2.8 ± 1
CEM/araC/C8							
G0/G1	49 ± 6	42 ± 6	58 ± 2	62 ± 4	43 ± 9	46 ± 0.9	46 ± 0.8
S-phase	46 ± 8	53 ± 7	40 ± 1	37 ± 4	54 ± 4	50 ± 0.6	50 ± 0.8
G2/M	5 ± 2	4.8 ± 3	4 ± 2	4 ± 1	3 ± 3	4 ± 1	7.7 ± 4
RL7							
G0/G1	46 ± 6	52 ± 10	58 ± 9	67 ± 0.4	65 ± 1	67.3 ± 3	68 ± 1
S-phase	44 ± 4	39 ± 8	40 ± 7	30 ± 1	32 ± 0.4	30 ± 1	29 ± 1
G2/M	8.9 ± 3	2.8 ± 1	4.8 ± 0.6	3.6 ± 0.8	3.7 ± 1	2.7 ± 1	3.4 ± 0.6
RL/G							
G0/G1	40 ± 8	40 ± 0.2	30 ± 6	28 ± 4	37 ± 0.1	68 ± 1.5	69 ± 10
S-phase	51 ± 8	52 ± 1	57 ± 5	62 ± 0.8	53 ± 4	31 ± 0.1	28 ± 9
G2/M	9 ± 4	8 ± 1	9.5 ± 2	9.8 ± 0.8	10 ± 4	7.2 ± 0.1	1.6 ± 1

[a] Cells were treated for 24 h with 1 μM of each compound. Values represent means ± SD of two separate experiments.

ment with both drugs, confirming the drug-resistant phenotype of these cells. In contrast, both sensitive and drug-resistant cell lines demonstrated high levels of apoptosis when treated with araCTP- and dFdCTP-containing nanogels. Thus, the cell growth inhibition observed in cytotoxicity assays was caused by an efficient induction of apoptosis in drug-resistant cells. NG2 was more efficient than NG1 in CEM and CEM/araC/C8 cells, while no difference was observed in RL7 and RL7/G cells. Nanogels without drugs induced low enough levels of apoptosis to conclude the lack of any toxicity associated with nanocarriers.

3.6. In vivo tumor xenograft model experiments

A subcutaneous tumor xenograft animal model of drug-resistant human follicular lymphoma cells was established in athymic *nu–nu* mice (Charles River Laboratories, Wilmington, MA). RL7/G cells (5×10^6 per injection) were suspended in 20% Matrigel (BD Bioscience, San Jose, CA) and administered *s.c.* into the low left flanks of mice (age of 5–6 weeks). Palpable tumors developed in as soon as 2 weeks and grew at a fast rate. All animal experiments were performed in accordance to institutional IACUC protocols and recommendations.

Initially, the efficacy of nanogel decoration with tumor lymphatic-specific LyP1 peptide was evaluated for *in vivo* targeting of xenografted tumors following *i.v.* administration. Nanogel NG1 was selected for *in vivo* experiments because of its lower intrinsic toxicity compared to NG2. The nanogel and its peptide derivatives (LyP1-NG1) with modification degrees of 1, 2, and 4% were loaded with the tritium-labeled model drug, ^{3}H-thymidine 5′-triphosphate, and then injected in the tail vein of tumor-bearing mice. Results of tumor accumulation measured 16 h later are shown in Fig. 3A. Initial nanogel accumulation in *s.c.* tumors (350–700 mm^3) was rather low and corresponded to 0.9 ± 0.4% ID/g. Peptide-modified nanogels demonstrated the most efficient tumor accumulation at 4% substitution rate, with a nearly 7-fold increase over non-modified nanogel (equivalent to 6% ID/g). Lower LyP1 substitution rates resulted in less efficient or no tumor-specific targeting of peptide-decorated nanogels. Thus, the LyP1 peptide seems to be useful for nanogel vectorization, showing an efficient lymphogenic tumor targeting *in vivo* at the relatively low number of peptides on the nanogel surface (ca. 40–60 molecules per nanogel).

Next, we examined tumor growth inhibition activity of dFdCTP-nanogels in the *s.c.* RL7/G xenograft animal model. Gemcitabine was *i.v.* injected twice a week in dose of 12 mg/kg, which is a half of clinically recommended dose of 1000 m^2 per week (Pestieau et al., 1998). Tumor-targeted LyP-NG1-dFdCTP and non-targeted NG1-dFdCTP nanogels were administered in dose of 60 mg/kg corresponding to the maximal tolerated *i.v.* dose (MTD) of cationic nanogels (Vinogradov et al., 2004). Median tumor volume changes in the control and treated groups are shown in Fig. 3B. Administration of gemcitabine did not induce any growth inhibition as compared to the control group. The tumor volume difference between gemcitabine and NG1-dFdCTP groups was moderate, but statistically significant. These data confirm the ability of circulating non-targeted nanogels to accumulate in the tumor mass, evidently because of the effect of enhanced permeability (Maeda et al., 2000). Nanogels decorated with multiple LyP1 peptide molecules (4 wt%) demonstrated a high tumor growth inhibitory effect that was statistically significant compared to the control and naked nanogel groups ($P < 0.0001$ and $P < 0.01$). The observed difference in tumor volume was approximately 3-fold between treated and control groups (Fig. 3B). All these data indicate that an efficient tumoral and cellular delivery of phosphorylated nucleoside analogs encapsulated in nanocarriers is able to overcome the drug resistance of cancer cells developed in the result of previous chemotherapy and to induce efficient growth inhibition of drug-resistant tumors.

Table 4
Levels of apoptosis in regular and drug-resistant cancer cells after treatment with nucleoside analogs or triphosphate drug-loaded nanoformulations.

Drug/formulation	CEM	CEM/araC/C8	RL7	RL7/G
Control	3 ± 0.7	3 ± 1	9 ± 3	13 ± 1
araC	50 ± 0.4	4 ± 1	32 ± 10	17 ± 0.8
NG1-araCTP	53 ± 0.8	38 ± 0.7	42 ± 9	37 ± 2
NG2-araCTP	67 ± 0.9	46 ± 0.9	37 ± 4	37 ± 2
dFdC	45 ± 0.4	5 ± 0.4	41 ± 0.7	22 ± 2
NG1-dFdCTP	44 ± 0.7	78 ± 1	39 ± 3	38 ± 1
NG2-dFdCTP	59 ± 1	84 ± 2	37 ± 0.7	39 ± 0.4

Apoptosis was measured in treated cells (1 μM drug, 24 h) using Annexin-V method (flow cytometry). Values represent means ± SD of two separate experiments.

4. Discussion

The application of activated phosphorylated nucleoside analogs and their prodrugs as anticancer therapeutics is slowly gaining popularity after the initial success of Fludara, having other phosphorylated drugs in pre-clinical phase. In the general sense, an optimal drug form for these compounds has to protect the phosphate moiety from degradation after administration, enhanced intracellular delivery, and then be efficiently converted into an

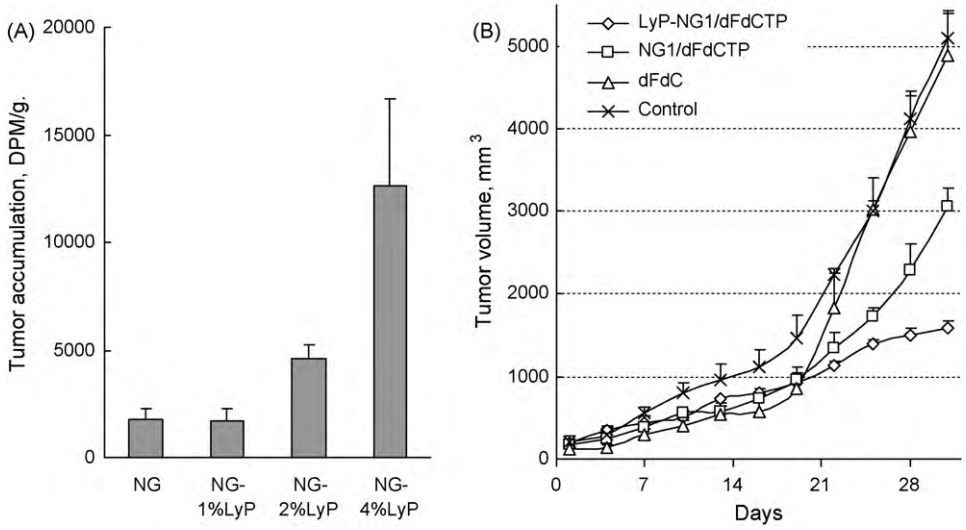

Fig. 3. Drug accumulation and tumor growth inhibition in drug-resistant tumors. (A) Accumulation of [^{3}H]-CTP in subcutaneous RL7/G tumors after the treatment with LyP1 peptide-decorated nanoformulations. The model drug was loaded into nanogels with various degrees of modification with LyP1 peptide. Equal doses of nanogel-[^{3}H]-CTP (0.3 μCi) were *i.v.* injected in RL7/G tumor-bearing nude mice, and the tumor-associated radioactivity was measured 16 h later. Data are shown as means ± SEM (n = 5). (B) Tumor growth inhibition in drug-resistant RL7/G xenograft mouse model. Doses of gemcitabine (12 mg/kg) and dFdCTP-loaded NG1 nanogels (60 mg/kg) were *i.v.* injected twice a week. Data are shown as means ± SEM (n = 5). P values: >0.05 (dFdC/control), <0.001 (NG1-dFdCTP/control), <0.0001 (LyP-NG1-dFdCTP/control), and <0.01 (NG1-dFdCTP/LyP-NG1-dFdCTP).

active free drug. All these goals are most easily achieved by using the nanoformulated drug delivery approach. During the last 15 years, many types of nanocarriers have been evaluated with various rates of success in the delivery of phosphorylated nucleotide analogs and NATP. Nanocapsules, nanoparticles, liposomes, and even red blood cells have been reported as being effective carriers for NATP, mostly as anti-HIV drugs (Hillaireau et al., 2006, 2007; Oussoren et al., 1999; Saiyed et al., 2009; Fraternale et al., 1996). Cationic nanogel networks have been initially introduced as a delivery system for anionic molecules (Vinogradov et al., 2002). Soft nanogel networks formed nanosized particles with core-shell structure and excellent dispersion stability after binding NATP molecules in aqueous media (Fig. 4). Nanogels also significantly enhanced nuclease stability and drug accumulation in cancer cells. Different NATP obtained from fludarabine, cytarabine, floxuridine, and zidovudine and encapsulated in nanogels demonstrated an enhanced drug activity, sometimes outperforming free drugs in many times (Vinogradov, 2007). Recently, we demonstrated that NATP-nanogels, being effective against a panel of human breast and colorectal cancer cell lines *in vitro*, were able to suppress the growth of human breast carcinoma *in vivo* (Galmarini et al., 2008b). The efficacy of the nanogel-triphosphate strategy was additionally tested through several examples of antiviral therapy using triphosphates of ribavirin against influenza A virus, or zidovudine and didanosine against HIV-1 in cell culture models (Kohli et al., 2007; Makarov et al., 2009).

In this study, we showed a strong potential of nanoformulations containing active triphosphates of cytarabine and gemcitabine in overcoming the drug resistance of cancer cells. Our results show that the observed increase in cytotoxic activity of NATP-nanogels in drug-resistant cells was principally due to the more efficient induction of apoptosis compared to parental drugs. As previously reported, the higher drug resistance of CEM/araC/C8 and RL7/G cell lines to cytarabine and gemcitabine, as compared to regular cell lines, was related to the lower level of apoptosis (Galmarini et al., 2003). In contrast, NATP-loaded nanoformulations induced equally high levels of apoptosis in both regular and drug-resistant cancer cells. However, these effects could vary for different nanocarriers

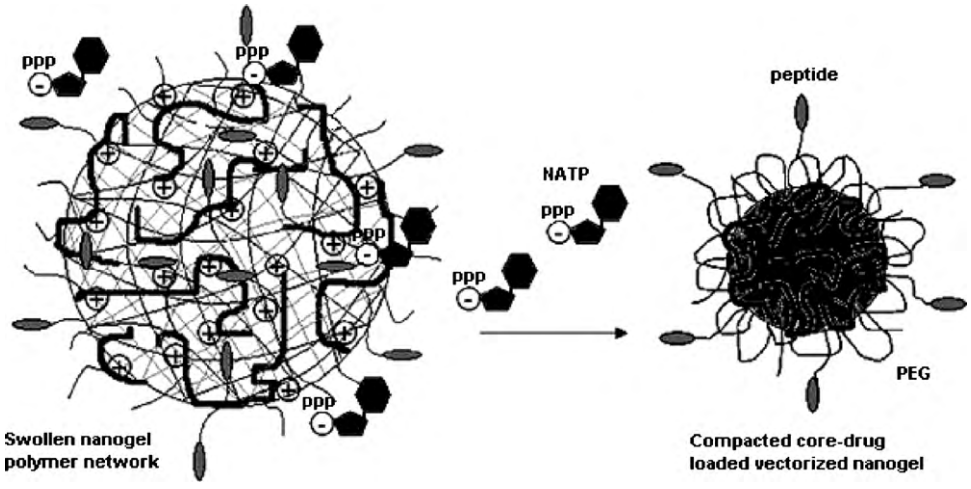

Fig. 4. Cationic network of the nanogel decorated with multiple small tumor-specific peptide ligands is capable to attract oppositely charged triphosphate drug molecules from aqueous solution and bind them with a formation of compact drug nanoformulations for systemic administration.

or cell lines. For example, drug-resistant cells lines are different by underlying mechanisms of drug resistance. CEM/araC/C8 cells are deficient by drug transporter activity, but have a normal level of drug activation, while RL/G cells have deficient drug activation in particular. We studied here two types of nanogels for drug delivery, NG1 and NG2, PEG- and Poloxamer-based cationic carriers, respectively. NG2 (P407-*cl*-SS-PEI) contains a hydrophobic core of Poloxamer P407 and, previously, showed a higher binding affinity to cellular membranes and better intracellular accumulation and triphosphate delivery than NG1 (PEG-*cl*-SS-PEI) (Vinogradov et al., 2006a). Here, it was more active in CEM and CEM/araC/C8 cells, but not in RL7 and RL/G cells, where drug activation, not transport, was the activity-limiting step. These features can partially explain the observed differences in activity. However, other factors, such as surface charge, or PEG density, or particle size could be of effect too.

Our data demonstrated the intracellular availability of active drugs (araCTP and dFdCTP) or their metabolites, inducing cell cycle arrest and consequent cell death. The functional evidence of the efficient intracellular delivery of nanogel-encapsulated NATP and later drug release was confirmed by direct HPLC analysis of NATP in the total cellular triphosphate pool. We did not detect any formation of a deoxyuridine metabolite of dFdCTP, the product of fast cellular deamination of gemcitabine, usually observed in treated patients (Giovannetti et al., 2008). The cell cycle showed a low response to nucleoside analogs in drug-resistant cells, while it became similar to drug-treated sensitive cancer cells following the treatment with NATP-nanogels. Our findings also suggest some nanocarrier-specific differences between drugs and nanoformulations in the cumulative effect on the cell cycle were probably associated with the fate of nanogels inside cancer cells, or with a strong imbalance in the triphosphate pool that could affect the efficacy of DNA polymerases.

Systemic drug delivery requires efficient targeting of nanocarriers to cancer cells. In order to determine how vectorized nanogels can be rated *in vivo*, we used a previously established subcutaneous gemcitabine-resistant human follicular lymphoma RL7/G xenograft mouse model (Galmarini et al., 2004). Previously evaluated EGFR-specific peptide, used in the surface decoration of nanogels, efficiently targeted human breast carcinoma in a xenograft model (Galmarini et al., 2008b), but unfortunately demonstrated low efficacy in this model. Therefore, we selected another short peptide, LyP1 that was found to be capable of binding with tumor lymphatics (Laakkonen et al., 2002). The target protein for LyP1 peptide is known as p32 and is overexpressed in tumor cells, on the surface of tumor lymphatics, and in myeloid cells, all contributing to the specificity of LyP1 homing (Fogal et al., 2008). Our assumption was that LyP1-vectorized nanocarriers could better target lymphogenic and poorly vascularized tumors. LyP1-decorated nanogels have been efficiently internalized by RL7/G cells *in vitro* and also accumulated in RL7/G xenografts *in vivo*. The peptide effect directly depended upon the degree of nanogel surface decoration. The tumor-targeting LyP1-NG1 nanogel was very efficient in the delivery of activated drugs into xenografted tumors and, as a result, it was selected for the treatment of gemcitabine-resistant RL7/G tumors. Repeated *i.v.* injections of nanoencapsulated dFdCTP induced significant tumor growth inhibition ($P < 0.05$) in the xenograft model. However, the LyP1-decorated nanogel was especially effective in this treatment ($P < 0.001$). Two other examples of successful tumor targeting using surface decoration with LyP1 have been recently reported for biodegradable polymeric and albumin nanoparticles (Karmali et al., 2009; Luo et al., 2009). Although several approaches of fighting drug resistance using vectorized nanocarriers are currently under investigation (Das et al., 2009), our results demonstrate the first example of the successful overcoming of drug resistance to anticancer nucleoside analogs using NATP nanoformulations. Delivery of phosphorylated nucleoside analogs in vectorized nanogels also presents an evident advantage, because it averts the cytopathic effects of chemotherapy in cases of recurrent tumors by reducing effective drug concentrations. Further improvements in anticancer efficacy can be expected along with the application of nanocarriers simultaneously carrying two anticancer drugs, e.g. paclitaxel and an activated nucleoside analog. Our preliminary data indicate that encapsulation of paclitaxel in a hydrophobic Pluronic core and binding of cytotoxic NATP in the cationic part of amphiphilic nanocarriers similar to NG2 used in the study could induce synergy in the cytotoxic activity of both drugs and be used for more efficient suppression of cancer growth (Vinogradov et al., 2008).

In conclusion, our data demonstrated that nanoformulations containing active triphosphates of nucleoside analogs were able to efficiently reverse the drug-resistant phenotype of lymphogenic cancer cells caused by deficient membrane nucleoside transport or dCK deficiency. Tumor-targeted nanocarriers displayed enhanced growth inhibition of drug-resistant tumors that were insensitive to therapeutic doses of gemcitabine. This strategy offers an opportunity for the treatment of cancer patients with relapse, and those who do not respond to conventional chemotherapy by cytotoxic nucleoside analogs. Given the potency of NATP-nanogel formulations against drug-resistant cancers, further studies will help to evaluate the full extent of the therapeutic potential of these nanoformulations as antitumor agents.

Acknowledgements

This work was supported in part by National Cancer Institute grant CA136921 to Serguei V. Vinogradov. Authors are very grateful to Trevor Gerson for his excellent technical assistance and help in the preparation of this manuscript. The contents of this study are solely the responsibility of the authors and do not necessarily represent the official views of the institute mentioned above.

References

Das, M., Mohanty, C., Sahoo, S.K., 2009. Ligand-based targeted therapy for cancer tissue. Expert Opin. Drug Deliv. 6, 285–304.
Diab, R., Degobert, G., Hamoudeh, M., Dumontet, C., Fessi, H., 2007. Nucleoside analogue delivery systems in cancer therapy. Expert Opin. Drug Deliv. 4, 513–531.
Ewald, B., Sampath, D., Plunkett, W., 2008. Nucleoside analogs: molecular mechanisms signaling cell death. Oncogene 27, 6522–6537.
Fogal, V., Zhang, L., Ruoslahti, E., 2008. Mitochondrial/cell surface protein p32/gC1qR as a molecular target in tumor cells and tumor stroma. Cancer Res. 68, 7210–7218.
Fraternale, A., Casabianca, A., Rossi, L., Chiarantini, L., Brandi, G., Aluigi, G., Schiavano, G.F., Magnani, M., 1996. Inhibition of murine AIDS by combination of AZT and dideoxycytidine 5′-triphosphate. J. Acquir. Immune Defic. Syndr. Hum. Retrovirol. 12, 164–173.
Galmarini, C.M., Jordheim, L., Dumontet, C., 2003. Pyrimidine nucleoside analogs in cancer treatment. Expert Rev. Anticancer Ther. 3, 717–728.
Galmarini, C.M., Clarke, M.L., Jordheim, L., Santos, C.L., Cros, E., Mackey, J.R., Dumontet, C., 2004. Resistance to gemcitabine in a human follicular lymphoma cell line is due to partial deletion of the deoxycytidine kinase gene. BMC Pharmacol. 4, 8.
Galmarini, C.M., Popowycz, F., Joseph, B., 2008a. Cytotoxic nucleoside analogues: different strategies to improve their clinical efficacy. Curr. Med. Chem. 15, 1072–1082.
Galmarini, C.M., Warren, G., Kohli, E., Zeman, A., Mitin, A., Vinogradov, S.V., 2008b. Polymeric nanogels containing the triphosphate form of cytotoxic nucleoside analogues show antitumor activity against breast and colorectal cancer cell lines. Mol. Cancer Ther. 7, 3373–3380.
Giovannetti, E., Laan, A.C., Vasile, E., Tibaldi, C., Nannizzi, S., Ricciardi, S., Falcone, A., Danesi, R., Peters, G.J., 2008. Correlation between cytidine deaminase genotype and gemcitabine deamination in blood samples. Nucleosides Nucleotides Nucleic Acids 27, 705–720.
Hillaireau, H., Le Doan, T., Appel, M., Couvreur, P., 2006. Hybrid polymer nanocapsules enhance in vitro delivery of azidothymidine-triphosphate to macrophages. J. Control. Release 116, 346–352.
Hillaireau, H., Le Doan, T., Chacun, H., Janin, J., Couvreur, P., 2007. Encapsulation of mono- and oligo-nucleotides into aqueous-core nanocapsules in presence of various water-soluble polymers. Int. J. Pharm. 331, 148–152.

Huber-Ruano, I., Pastor-Anglada, M., 2009. Transport of nucleoside analogs across the plasma membrane: a clue to understanding drug-induced cytotoxicity. Curr. Drug Metab. 10, 347–358.
Jordheim, L., Galmarini, C.M., Dumontet, C., 2003. Drug resistance to cytotoxic nucleoside analogues. Curr. Drug Targets 4, 443–460.
Jordheim, L.P., Cros, E., Gouy, M.H., Galmarini, C.M., Peyrottes, S., Mackey, J., Perigaud, C., Dumontet, C., 2004. Characterization of a gemcitabine-resistant murine leukemic cell line: reversion of in vitro resistance by a mononucleotide prodrug. Clin. Cancer Res. 10, 5614–5621.
Jordheim, L.P., Galmarini, C.M., Dumontet, C., 2006. Gemcitabine resistance due to deoxycytidine kinase deficiency can be reverted by fruitfly deoxynucleoside kinase, DmdNK, in human uterine sarcoma cells. Cancer Chemother. Pharmacol. 58, 547–554.
Karmali, P.P., Kotamraju, V.R., Kastantin, M., Black, M., Missirlis, D., Tirrell, M., Ruoslahti, E., 2009. Targeting of albumin-embedded paclitaxel nanoparticles to tumors. Nanomedicine 5, 73–82.
Kohli, E., Han, H.Y., Zeman, A.D., Vinogradov, S.V., 2007. Formulations of biodegradable Nanogel carriers with 5′-triphosphates of nucleoside analogs that display a reduced cytotoxicity and enhanced drug activity. J. Control. Release 21, 19–27.
Laakkonen, P., Porkka, K., Hoffman, J.A., Ruoslahti, E., 2002. A tumor-homing peptide with a targeting specificity related to lymphatic vessels. Nat. Med. 8, 751–755.
Lutsenko, S.V., Feldman, N.B., Severin, S.E., 2002. Cytotoxic and antitumor activities of doxorubicin conjugates with the epidermal growth factor and its receptor-binding fragment. J. Drug Target. 10, 567–571.
Luo, G., Yu, X., Jin, C., Yang, F., Fu, D., Long, J., Xu, J., Zhan, C., Lu, W., 2009. LyP-1-conjugated nanoparticles for targeting drug delivery to lymphatic metastatic tumors. Int. J. Pharm. (epub October 13).
Maeda, H., Wu, J., Sawa, T., Matsumura, Y., Hori, K., 2000. Tumor vascular permeability and the EPR effect in macromolecular therapeutics: a review. J. Control. Release 65, 271–284.
Makarov, E., Gerson, T., Poluektova, L., Vinogradov, S.V., 2009. Efficient suppression of human immunodeficiency virus in macrophages by Nano-NRTIs, Abstract 7th International Nanomedicine and Drug Delivery Symposium, Indianapolis, USA, p. 92.
Meier, C., Balzarini, J., 2006. Application of the cycloSal-prodrug approach for improving the biological potential of phosphorylated biomolecules. Antiviral Res. 7, 282–292.
Nori, A., Kopecek, J., 2005. Intracellular targeting of polymer-bound drugs for cancer chemotherapy. Adv. Drug Deliv. Rev. 57, 609–636.
Oussoren, C., Magnani, M., Fraternale, A., Casabianca, A., Chiarantini, L., Ingebrigsten, R., Underberg, W.J., Storm, G., 1999. Liposomes as carriers of the antiretroviral agent dideoxycytidine-5'-triphosphate. Int. J. Pharm. 180, 261–270.
Pestieau, S.R., Stuart, O.A., Chang, D., Jacquet, P., Sugarbaker, P.H., 1998. Pharmacokinetics of intraperitoneal gemcitabine in a rat model. Tumori 84, 706–711.
Peyrottes, S., Egron, D., Lefebvre, I., Gosselin, G., Imbach, J.L., Périgaud, C., 2004. SATE pronucleotide approaches: an overview. Mini Rev. Med. Chem. 4, 395–408.
Saiyed, Z.M., Gandhi, N.H., Nair, M.P., 2009. AZT 5'-triphosphate nanoformulation suppresses human immunodeficiency virus type 1 replication in peripheral blood mononuclear cells. J. Neurovirol. 2, 1–5.
Twentyman, P.R., Fox, N.E., Rees, J.K., 1989. Chemosensitivity testing of fresh leukaemia cells using the MTT colorimetric assay. Br. J. Haematol. 71, 19–24.
Ullman, B., 1989. Dideoxycytidine metabolism in wild type and mutant CEM cells deficient in nucleoside transport or deoxycytidine kinase. Adv. Exp. Med. Biol. 253B, 415–420.
Vinogradov, S.V., Bronich, T.K., Kabanov, A.V., 2002. Nanosized cationic hydrogels for drug delivery: preparation, properties and interactions with cells. Adv. Drug Deliv. Rev. 54, 135–147.
Vinogradov, S.V., Batrakova, E.V., Kabanov, A.V., 2004. Nanogels for oligonucleotide delivery to the brain. Bioconjug. Chem. 15, 50–60.
Vinogradov, S.V., Zeman, A.D., Batrakova, E.V., Kabanov, A.V., 2005a. Polyplex Nanogel formulations for drug delivery of cytotoxic nucleoside analogs. J. Control. Release 107, 143–157.
Vinogradov, S.V., Kohli, E., Zeman, A.D., 2005b. Cross-linked polymeric nanogel formulations of 5'-triphosphates of nucleoside analogues: role of the cellular membrane in drug release. Mol. Pharm. 2, 449–461.
Vinogradov, S.V., Kohli, E., Zeman, A.D., 2006a. Comparison of nanogel drug carriers and their formulations with nucleoside 5'-triphosphates. Pharm. Res. 23, 920–930.
Vinogradov, S.V., Kohli, E., Zeman, A., Kabanov, A.V., 2006b. Chemical engineering of nanogel drug carriers: increased bioavailability and decreased cytotoxicity. Polymer Prepr. (ACS) 47, 27–28.
Vinogradov, S.V., 2007. Polymeric nanogel formulations of nucleoside analogs. Expert Opin. Drug Deliv. 4, 5–17.
Vinogradov, S.V., Mitin, A., Warren, G., 2008. Folate-targeted polyformulations of cytotoxic nucleoside triphosphates and paclitaxel. Polymer Prepr. (ACS) 49, 1050–1051.